Interfacial Modification through End Group Complexation in Polymer Blends

Cathy A. Fleischer,† Ana Rita Morales,‡ and Jeffrey T. Koberstein*

Institute of Materials Science and Department of Chemical Engineering, University of Connecticut, Storrs, Connecticut 06269-3136

Received May 26, 1993; Revised Manuscript Received October 22, 1993®

ABSTRACT: The concept of interpolymer complexation is applied to develop a new method for interfacial modification of immiscible binary homopolymer blends. In this method, end-functional homopolymers terminated with acid and base groups are added to the blend to promote in situ end-complexation of the immiscible materials across the interface. More specifically, carboxy-terminated polybutadiene and amine-terminated poly(dimethylsiloxane) are employed to compatibilize an immiscible blend of polybutadiene and poly(dimethylsiloxane). The interpolymer complex that forms between acid and base groups creates a "block-copolymer-like" structure that spans across the interface. Pendant drop tensiometry is applied to measure the interfacial tension reduction afforded by this complexation. The interfacial tension data show behavior similar to that observed for block copolymer addition to homopolymer blends: there is initially a linear decrease of interfacial tension with the concentration of functional homopolymer up to a critical concentration at which the interfacial tension becomes invariant to further increases in the concentration of functional material. In contrast to the behavior of block copolymers, however, the formation of interpolymer complexes is dependent on the equilibrium between associated and dissociated functional groups. That is, the ultimate plateau value for interfacial tension reduction is dependent on the functional group stoichiometry. A reaction model for end-complexation is developed including the effects of carboxylic acid dimerization in order to reproduce the interfacial tension reduction data. Fourier transform infrared spectroscopy is applied to determine the appropriate rate constants. The model provides a reasonable qualitative description of the interfacial tension results but cannot quantitatively predict the critical compositions observed experimentally. Finally, it is shown that the overall interfacial tension behavior is consistent with that predicted by current statistical thermodynamic theories developed for block copolymers.

Introduction

The control of interfacial tension in immiscible polymer blends is important, due to its role in governing the blend morphology and associated mechanical properties. As interfacial tension is reduced, the dispersed phase particle size is also reduced, as defined by the Weber number.[1] Reducing the dispersed phase size is important for obtaining uniform blend properties while retaining the physical properties of both of the homopolymers.

It is well known that block and graft polymers are efficient additives for the reduction of polymer/polymer interfacial tension.[2-5] In work by Patterson, Hu, and Grindstaff,[2] Gaillard, Ossenbach-Sutter, and Reiss,[3] and Anastasiadis, Gancarz, and Koberstein,[4] addition of only 2% of a copolymer, comprising species identical to those of the two immiscible homopolymers in the blend, resulted in an interfacial tension reduction of 40–70%.

The incorporation of block copolymers into immiscible polymer blends brings an added benefit of increased adhesion[5,6] due to chain entanglement and bridging across the interface. By including the diblock copolymer, both yield strength and ultimate elongation are increased, illustrating the synergy of properties possible in immiscible polymer blends.[7]

However, there are also disadvantages and difficulties associated with the use of block copolymers as interfacial agents. The microphase separation inherent to most block copolymers leads to high viscosities, making it difficult to disperse them into binary homopolymer blends. In addition, high molecular weight block copolymers may prefer to micellize within one of the homopolymer phases rather than localize at the interface. Finally, block copolymers are often expensive and may not be available for all homopolymer pairs.

Many of the shortcomings of block copolymers can be avoided by forming block copolymers in situ. This usually is accomplished by processes such as reactive grafting, wherein reactive functional groups on the two homopolymers undergo an interfacial reaction to form a covalent bond between the chains in each phase.[8] The resulting graft copolymer behaves much like a block copolymer to decrease interfacial tension and increase adhesion, but forms directly at the interface. The mixing and micellization problems associated with block copolymer addition are therefore circumvented by formation of block copolymers in situ.

An interesting extension of this concept involves interpolymer complexation across the interface of immiscible blends. In the work of Russell, Jerome, Charlier, and Foucart,[9] dimethylamino end groups on polyisoprene were complexed with carboxylic acid or sulfonic acid end groups on polystyrene to form microphase-separated block-copolymer-like materials, as indicated by small-angle X-ray scattering (SAXS). At temperatures of 140–160 °C the carboxylic acid–tertiary amine complex was disrupted, and macrophase separation occurred. Sen, Weiss, and Garton[10] similarly formed graft copolymers by complexation of copper carboxylate-terminated polybutadiene with poly(styrene-*co*-4-vinylpyridine).

Complexation through hydrogen bonding[11-13] or ionic interactions[14,15] has been used extensively in polymer blends to enhance miscibility, as has been reviewed previously.[16-18] Many systems, for example, promote formation of ionic interpolymer complexes between sulfonate groups on one polymer and vinylpyridine groups

* To whom correspondence should be addressed.
† Present address: Eastman Kodak Co., Rochester, NY 14650-2104.
‡ Visiting Scientist from the University Federal of San Carlos, San Carlos, Brazil.
® Abstract published in *Advance ACS Abstracts,* December 1, 1993.

0024-9297/94/2227-0379$04.50/0

on the other.[14,15,19] Organic cations have also been used for complexation, as in the case of the neutralization of carboxylated polyethylene with ethylenediamine.[20,21] IR spectroscopy confirmed salt formation between the primary amine and the carboxylic acid.

In this paper, we apply the concept of interpolymer complexation to bring about interfacial modification of immiscible binary homopolymer blends. End-functional homopolymers with acid and basic functionality are added to the blend to promote the formation of "block-copolymer-like" interpolymer complexes across the interface. With this approach, problems associated with the high viscosity of block copolymers are eliminated, as the starting components have molecular weights similar to those of the homopolymers. In addition, the complexation process that occurs mimics the in situ grafting reactions that are employed in compatibilization strategies for reactive processing of immiscible blends.

Experimental Section

Materials. Polybutadiene (PBD) (M_n = 1500, M_w/M_n = 2.0) and carboxy-terminated polybutadiene (PBD–COOH) (M_n = 2000, M_w/M_n = 1.6) were obtained from Nissho Iwai American Corp., New York, NY. Poly(dimethylsiloxane) (PDMS) (M_n = 10000, M_w/M_n = 1.7) was obtained from Professor Judy Riffle of Virginia Polytechnic Institute. Difunctionally terminated (aminopropyl)poly(dimethylsiloxane) (PDMS–NH_2) was obtained from Thoratec Corp. (M_n = 1000) and Goldschmidt Chemical Corp. (M_n = 10000). Details of the synthesis are described elsewhere.[22] The PDMS–NH_2 from Goldschmidt Chemical Corp. was fractionated by supercritical fluid fractionation at Phasex Corp., Lawrence, MA, to obtain material with a M_n = 9600 and M_w/M_n = 1.5 using previously described procedures.[23] PDMS, PDMS–NH_2, PBD, and PBD–COOH were characterized by size exclusion chromatography (SEC), vapor phase osmometry (VPO), and end group titration. SEC of PDMS and PDMS–NH_2 was conducted using a Waters system[24] with toluene as a solvent. To avoid retention in the columns, PDMS–NH_2 was derivatized prior to SEC characterization by reacting excess phenyl isocyanate with the amine end groups. PBD and PBD–COOH SEC was conducted using THF as the solvent. VPO was conducted on a Wescan Model 233 system at 50 °C using toluene as the solvent. PDMS–NH_2 end group titration was carried out using a measured amount of PDMS in 2-propanol. Bromophenol blue was used as an indicator, and titration to a yellow end point was carried out using 0.1 N HCl from Fisher Scientific. It was assumed that PDMS–NH_2 had exactly two end groups per chain. PBD–COOH end group titration was carried out using a measured amount of PBD–COOH in MEK. Phenolphthalein was used as an indicator, and titration to a violet end point was conducted using 0.1 N KOH from Fisher Scientific. A blank containing an equivalent amount of solvent was titrated similarly and subtracted from the PBD–COOH results.

Methods. Interfacial tension measurements were made by pendant drop tensiometry using a system for digital analysis of pendant drop images similar to that described previously.[25,26] The experimental drop profile is compared to the theoretical profile as predicted by the equations of Bashforth and Adams.[27] A robust shape comparison algorithm that has been modified to include a golden section optimization[28] is used to determine the shape parameter and the magnification factor for the resulting drop profile, which is related to the interfacial tension value.

A drop of a PDMS/PDMS–NH_2 mixture was formed using a 10-μL Drummond syringe in a matrix of PBD/PBD–COOH contained in a 1-cm glass cuvette. The cuvette was placed in a chamber controlled to 30 ± 1 °C. The observed image was digitized and thresholded to obtain the drop profile using an AT&T TARGA image capture board. A 0.5 mm × 0.5 mm grid was analyzed for calibration of the magnification factor. Images were obtained and analyzed at regular intervals until a constant, equilibrium result was obtained. The drop volume was then increased, and the same procedure repeated.

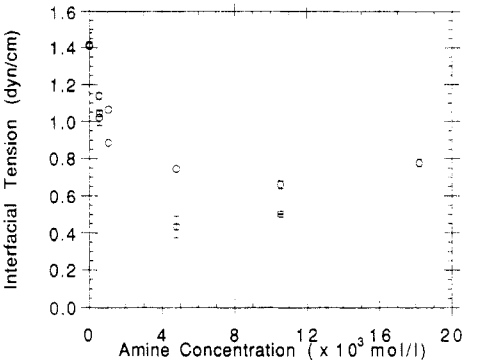

Figure 1. Interfacial tension vs NH_2 concentration for immiscible blends of PBD/PBD–COOH mixtures with PDMS/PDMS–NH_2: (○) 4.88 × 10^{-3} mol/L COOH; (□) 2.4 × 10^{-2} mol/L COOH.

Density measurements, necessary for interfacial tension measurements, were conducted at 30 °C using an Anton Paar K.G. Model DMA 60 digital density meter, with external cell model DMA 602. Temperature precision of ±0.1 °C was obtained with a water bath.

Model equilibrium complex concentrations were determined by solving two nonlinear simultaneous equations using a software program, NONLIN, developed by Cutlip and Shacham at the University of Connecticut.[29] Fourier transform infrared spectroscopy (FTIR) was conducted using a heated cell with rectangular NaCl salt plates and a 0.015-mm spacer. The PBD–COOH was used for determining the dimerization equilibrium constant. For determination of the amine–carboxylic acid equilibrium constant, a 1:1 molar ratio of amine:acid end groups was used, as determined by end group titration for the PDMS–NH_2 and PBD–COOH samples (65 wt % PBD–COOH). The materials were blended for a minimum of 1 h at 40 °C prior to filling the IR cell and were completely miscible as judged by their transparency. The concentration of COOH end groups in the PBD–COOH is 9.84 × 10^{-4} mol/g, and the concentration of NH_2 end groups in the PDMS–NH_2 (M_n = 1000) is 1.98 × 10^{-3} mol/g, as determined by the end group titration methods described above.

FTIR spectra were collected on a Nicolet 60SX spectrophotometer using a TGS detector. Thirty-two scans were averaged, and the resolution was 4 cm^{-1}. Spectra were obtained for temperatures ranging from room temperature to 120 °C. Resolution of the carbonyl spectral region was accomplished by curve fitting using the Spectra Calc analysis package. Water was subtracted from the spectra, and the baseline was corrected using standard procedures. Density was measured as a function of temperature for the PBD–COOH and the PBD–COOH/PDMS–NH_2 blend, so that accurate molar concentrations could be obtained for the temperature range of interest.

Results and Discussion

Interfacial Tension Results. The interfacial tension of the PDMS/PDMS–NH_2/PBD/PBD–COOH blends as a function of NH_2 concentration for two different COOH concentrations is presented in Figure 1. The results show that the interfacial tension decreases linearly as the end group concentration increases and then reaches a plateau at higher end group concentrations. Interfacial tension reduction of up to 70% is observed for this system. Similar results are observed when the amine concentration is held constant, while increasing the COOH concentration (Figure 2). The linear interfacial tension reduction observed at low concentrations is more evident with the expanded scale of Figure 3. Similar interfacial tension reduction was observed by Anastasiadis, Gancarz, and Koberstein upon addition of block copolymer to an immiscible polymer blend.[4] Addition of poly(styrene-*b*-butadiene) to the PS/PBD immiscible polymer blend resulted in a linear

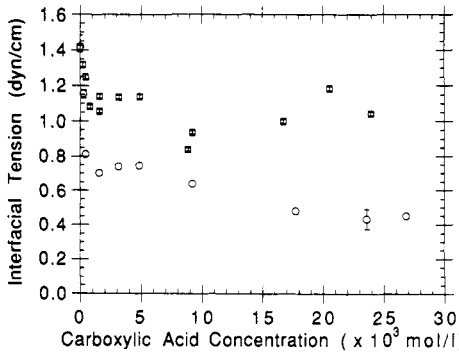

Figure 2. Interfacial tension vs COOH concentration ((0–30.0) × 10^{-3} mol/L) for immiscible blends of PBD/PBD–COOH with PDMS/PDMS–NH_2: (○) 4.8 × 10^{-3} mol/L NH_2; (□) 5.4 × 10^{-4} mol/L NH_2.

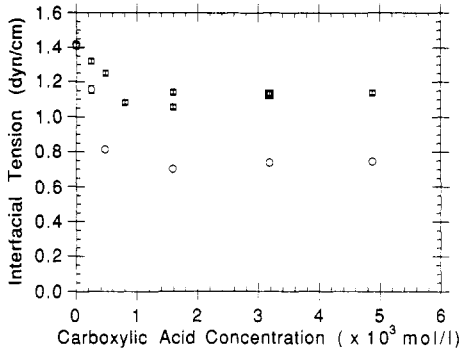

Figure 3. Interfacial tension vs COOH concentration ((0–6.0) × 10^{-3} mol/L) for immiscible blends of PBD/PBD–COOH with PDMS/PDMS–NH_2: (○) 4.8 × 10^{-3} mol/L NH_2; (□) 5.4 × 10^{-4} mol/L NH_2.

reduction in interfacial tension initially, followed by a plateau above a critical concentration, ϕ_{crit}. The plateau is typically attributed to attainment of the critical micelle concentration (cmc), a critical concentration above which the copolymer chains form micelles in the bulk, as opposed to going to the interface.

It was initially expected that the interfacial tension in the complexed system would reach the plateau value when a 1:1 ratio between the amine and acid end groups was obtained, such that further addition of amine or acid end groups would not result in further interfacial tension reduction. However, for the higher COOH (0.0048 and 0.024 mol/L) and NH_2 (0.0048 mol/L) concentrations, the interfacial tension data show a plateau below the 1:1 ratio at the cmc. In contrast, for the 0.00054 mol/L NH_2 concentration (Figure 3) the interfacial tension continues to drop beyond the 1:1 molar ratio, although this concentration is below the apparent critical concentration observed at higher end group concentrations. The plateau for these interpolymer complexes therefore appears to be associated with the complexation equilibrium, rather than a cmc.

In the PDMS–NH_2/PBD–COOH system, complexes can form between the amine and acid end groups or between two carboxylic acid end groups. The self-association of carboxylic acids to form dimers has been demonstrated for many small-molecule and polymeric systems.[30-32] As a result, additional COOH end groups may be needed beyond the 1:1 molar ratio to obtain maximal interpolymer complexation and interfacial tension reduction. This concept can be pursued further by modeling the interfacial reactions and complexation equilibria for the 5.4 × 10^{-4} mol/L NH_2 concentration.

Reaction Model Development. The major reactions occurring in the PDMS–NH_2/PBD–COOH system can be written as follows for the amine–acid and dimer complexes:

$$[A] + [B] \rightleftharpoons [C] \quad (1)$$

$$2[A] \rightleftharpoons [D] \quad (2)$$

If we define [A] as the carboxylic acid concentration, [B] as the amine concentration, [C] as the amine–acid complex concentration, and [D] as the acid–acid dimer concentration, the corresponding equilibrium constants for complex and dimer formation are for the amine–acid complex

$$K_c = \frac{[C]}{[A][B]} \quad (3)$$

and for the dimer

$$K_d = [D]/[A]^2 \quad (4)$$

Equations 3 and 4 can be written in terms of the initial concentrations of acid and base, $[A]_0$ and $[B]_0$, and the extents of reaction to form the complex and the dimer, x_c and x_d, respectively. The concentrations of carboxylic acid, amine, complex, and dimer would be as follows:

$$[A] = [A]_0(1 - x_c - x_d) \quad (5)$$

$$[B] = [B]_0 - [A]_0 x_c \quad (6)$$

$$[C] = [A]_0 x_c \quad (7)$$

$$[D] = {}^1/_2[A]_0 x_d \quad (8)$$

The following expressions are obtained for the equilibrium constants:

$$K_c = \frac{[A]_0 x_c}{[A]_0(1 - x_c - x_d)([B]_0 - [A]_0 x_c)} \quad (9)$$

$$K_d = \frac{{}^1/_2[A]_0 x_d}{[A]_0^2(1 - x_c - x_d)^2} \quad (10)$$

The unknowns in the equilibrium constants are the extents of reaction, x_c and x_d, and the two equilibrium constants, K_c and K_d.

Model curves are calculated for different equilibrium constant values to determine what complex concentrations would be predicted for different systems. In the work of MacKnight et al.,[30] the dimerization equilibrium constant was determined using infrared spectroscopy. They obtained a value of 3160 L/mol at 30 °C for ethylene–methacrylic acid copolymers. Using this value, the complex concentration as a function of acid or amine concentration is calculated for different amine–acid complex equilibrium constants.

Results are presented in Figure 4 for an NH_2 concentration of 5.4 × 10^{-4} mol/L for three complex equilibrium constants: $K_c = 10K_d$, $K_c = K_d$, and $K_c = 0.1K_d$. If the complex equilibrium constant is much smaller than the dimerization equilibrium constant, then the complex concentration continues to increase slowly far beyond the 1:1 molar ratio and will only reach one-third of the maximum concentration possible (5.4 × 10^{-4} mol/L), even for high acid concentrations. If the complex equilibrium constant is 10 times greater than the dimerization equilibrium constant, the maximum complex concentration (and thus minimum interfacial tension, assuming the concentration is below the critical concentration) is almost attained at a 1:1 molar ratio between the amine and acid end groups. When the equilibrium constants are equal, a significant amount of complexation occurs at high acid

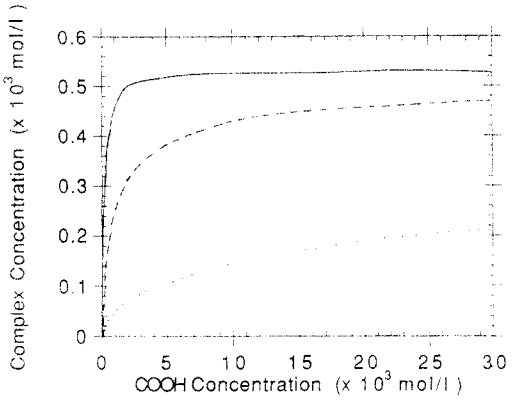

Figure 4. Complex reaction model results for blends of PBD/PBD–COOH mixtures with PDMS/PDMS–NH_2. Complex concentration vs COOH concentration ((0–30.0) × 10^{-3} mol/L) (K_d = 3162 L/mol): solid line, $K_c = 10K_d$; dashed line, $K_c = K_d$; dotted line, $K_c = 0.1K_d$.

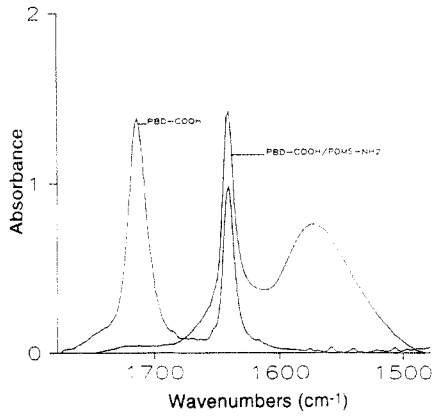

Figure 5. FTIR spectra of PBD–COOH and PBD–COOH/PDMS–NH_2 blend at 40 °C.

concentration, resulting in a complex concentration close to 90% of the maximum concentration.

As measured by Anastasiadis et al.[4] and predicted by mean field block copolymer immiscible blend theories of Hong and Noolandi,[33-35] an increase in block copolymer concentration results in a linear decrease in interfacial tension at low block copolymer concentrations (below the cmc). A linear decrease in interfacial tension would thus be predicted for interpolymer complexation across the interface as end group concentration increases. By comparison of the experimental interfacial tension data in Figures 2 and 3 with the model complex concentrations presented in Figure 4, the complex equilibrium constant may be estimated. The experimental data level off at a concentration of 1 × 10^{-3} mol/L COOH, which is similar to the critical concentration for the model curve for $K_c \simeq 10K_d$. This high equilibrium constant for the complex suggests that the complex is an ionic salt, as opposed to a hydrogen-bonded complex. The investigation of this possibility by infrared spectroscopy is described in the next section. In addition, experimental equilibrium constants are determined for the complex model equations for our specific system.

Equilibrium Constant Measurement Using FTIR. FTIR spectra for the PBD–COOH and the PBD–COOH/PDMS–NH_2 blend at 40 °C are presented in Figure 5. The spectra for PBD–COOH show a band at 1713 cm^{-1} corresponding to the bonded carbonyl, with a shoulder at 1752 cm^{-1} corresponding to the free carbonyl. The band at 1639 cm^{-1} is common to both spectra and is attributed to the unsaturated bonds in the PBD. The PBD–COOH/PDMS–NH_2 blend has negligible absorbance at 1713 cm^{-1}

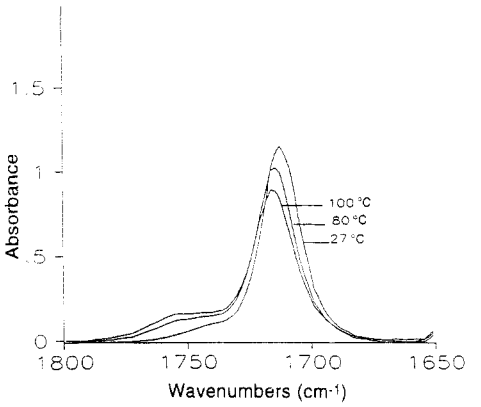

Figure 6. FTIR spectra of PBD–COOH at 27, 80, and 100 °C.

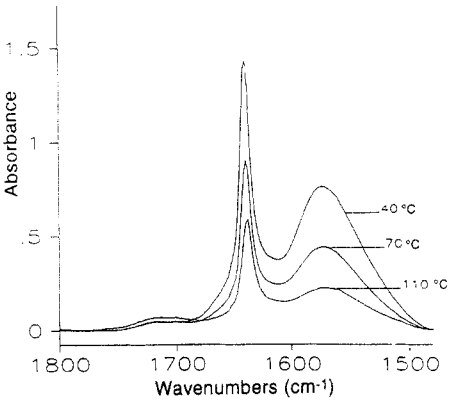

Figure 7. FTIR spectra of PBD–COOH/PDMS–NH_2 blend at 40, 70, and 110 °C.

for the hydrogen-bonded carbonyl and, instead, exhibits a broad band at 1570 cm^{-1} corresponding to the carboxylate salt, which is formed with the amine end group. This clearly shows that the complex formed is that of an ionic salt, as opposed to a hydrogen-bonded complex.

FTIR spectra of the PBD–COOH experiment for 27, 80, and 100 °C are presented in Figure 6. As would be expected, as temperature increases the bonded carbonyl band decreases in magnitude, while the free carbonyl band increases in magnitude.

Figure 7 presents the results of the PBD–COOH/PDMS–NH_2 experiment for a range of temperatures. At room temperature the carboxylate salt band at 1570 cm^{-1} is large, and there is negligible absorbance at 1710 cm^{-1}, where the bonded carbonyl would be expected. As temperature is increased, the carboxylate band decreases in strength and the bonded carbonyl band at 1705 cm^{-1} is observed. The band at 1640 cm^{-1} decreases with increasing temperature. The data were used to measure the concentrations of the species required as defined by eqs 3 and 4 for calculation of the equilibrium constants.

For the PBD–COOH dimerization experiment, peak areas were determined for the bonded or dimerized carbonyl bands at a wavenumber of 1712–1716 cm^{-1} and for the free carbonyl band at 1751–1754 cm^{-1}. The dimerization equilibrium constants were calculated following the method of MacKnight et al.[30] (See Appendix for details.)

For the PBD–COOH/PDMS–NH_2 experiment, peak areas were determined for the bonded carbonyl band at 1703–1707 cm^{-1} and for the carboxylate salt band in the range of 1569–1574 cm^{-1}. There was no measurable free acid present. The extinction coefficient for the carboxylate salt (ϵ_c) was determined at room temperature and at 40 °C, where the bonded carbonyl concentration was negligible. It was not possible to measure the amine concen-

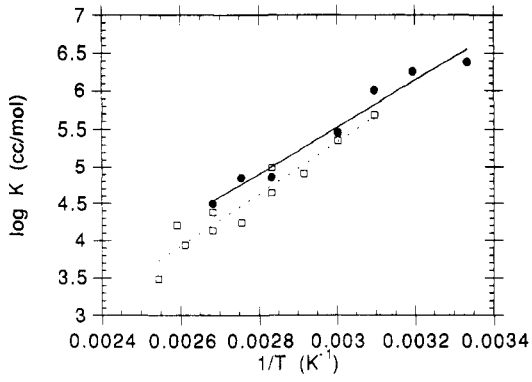

Figure 8. log K vs $1/T$ for (●) PBD–COOH dimerization constant (K_d) and (□) PBD–COOH/PDMS–NH_2 complex (K_c).

tration, as the band was not strong enough. Therefore, eqs 6 and 7 were combined and substituted for the amine concentration (B) in eq 3, resulting in the following:

$$K_c = \frac{[C]}{[A]([B]_0 - [C])} \tag{11}$$

where $[B]_0$ is the initial amine concentration. In addition, substitution of eq 4 into eq 3 results in

$$K_c = \frac{[C]K_d^{1/2}}{[D]^{1/2}([B]_0 - [C])} \tag{12}$$

so that K_c can be calculated from the dimer and complex concentrations measured by FTIR.

Figure 8 presents the results of the dimerization and amine–acid complex equilibrium constants plotted as log K vs $1/T$. The equation for the dimer equilibrium constant is

$$\log K_d = -3.780 + 3100/T \qquad R = 0.9818 \tag{13}$$

and the equation for the complex equilibrium constant is

$$\log K_c = -5.194 + 3507/T \qquad R = 0.9943 \tag{14}$$

The dimerization equilibrium constant measured at 30 °C, the temperature at which interfacial tension was measured, is 2800 L/mol, which is comparable to the value of 3160 L/mol which was measured by MacKnight for poly(acrylic acid) (PAA).[30] The results show that, at 30 °C, K_c is 2400 L/mol, approximately equal to K_d.

As shown in Figure 8, both equilibrium constants are 3 orders of magnitude smaller at 140 °C, as compared to 30 °C. Therefore, at elevated temperature complexation between amine and acid end groups would be small. This is consistent with observations of Russell et al. for carboxylic acid–tertiary amine complexes.[9] They observed that the complex dissociated at temperatures of 140–160 °C, as detected by SAXS.

The enthalpy of complex formation is calculated from the slope of the log K vs $1/T$ plot. The ΔH value calculated from the slopes of the dimerization experiment was −14.2 kcal/mol, which is a fairly reasonable value for the dimer bond strength. Typical hydrogen bond strengths range from −5 to −6 kcal/mol,[11,30] and a bond strength of twice that would be expected for a dimer which contains two hydrogen bonds. The ΔH value measured for the amine–acid complex is −16.0 kcal/mol.

PBD–COOH/PDMS–NH_2 Model Results. The equilibrium constants which were determined by FTIR are incorporated into the reaction model, resulting in the model curve shown in Figure 9 for an amine concentration of 5.4×10^{-4} mol/L. The increase in complex concentration beyond the 1:1 molar ratio is qualitatively consistent with

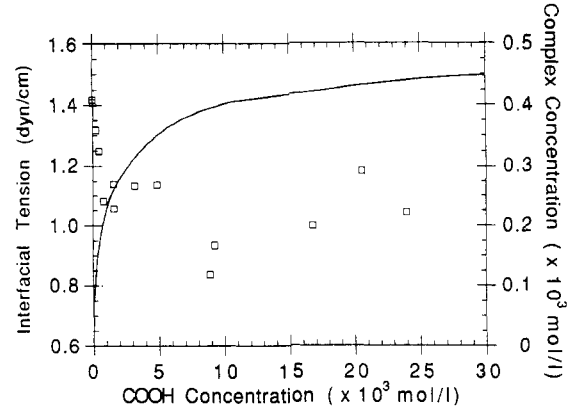

Figure 9. PBD–COOH/PDMS–NH_2 reaction model complex concentration using K_d = 2820 L/mol and K_c = 2400 L/mol (solid line) and interfacial tension data (□) vs COOH concentration for 5.4×10^{-4} mol/L NH_2.

the interfacial tension results. However, by comparison with the model curves in Figure 4, it is clear that the interfacial tension reaches a minimum at a lower COOH concentration, as compared to the model curve. The interfacial tension reaches a plateau at a COOH concentration of about 10^{-3} mol/L, whereas the complex concentration calculated by the model continues to increase to a COOH concentration of approximately 10^{-2} mol/L. The interfacial tension and the complex concentration were expected to plateau at the same concentration. However, the complex concentration is calculated from a bulk model, while neglecting other factors.

Discussion. The interfacial properties of polymer interfaces modified by the addition of block copolymers have been the subject of several theoretical treatments.[33-37] More recently, the effect of sequence distribution within the block copolymer and the effects of multiblock copolymers at interfaces have been investigated.[38]

For systems of two homopolymers and a diblock copolymer containing blocks of the two polymers,[34] the interfacial tension was calculated as a function of block copolymer concentration and the resulting homopolymer and copolymer concentration profiles. Subsequent computer simulations led to development of the following simplified equation for a symmetrical system with homopolymers of infinite molecular weight:[35]

$$\Delta\gamma = d\phi_c\left[({}^1/_2\chi_{AB} + 1/Z_c) - \frac{1}{Z_c}e^{Z_c\chi_{AB}/2}\right] \tag{15}$$

where Z_c is the degree of polymerization of the copolymer blocks, assumed equal, ϕ_c is the copolymer volume fraction, and d is the interfacial width at half-height, red uced by the Kuhn length. The values for Z_c, χ_{AB}, and d are constants for our system of end-complexed "block copolymers", so the interfacial tension reduction should increase linearly with the copolymer (i.e., complex) concentration.

Equation 15 does not consider the effects of micellization and can only be applied to our system for concentrations below the cmc. The reaction model was used to calculate the amine–acid complex concentration in the bulk. The complex concentration defines the volume fraction of the block copolymer present, as is required in eq 15. The volume fraction can be calculated from the following equation:

$$\phi_c = [C]\left(\frac{MW_A}{\rho_A} + \frac{MW_B}{\rho_B}\right) \tag{16}$$

where [C] is the complex concentration in mol/L, polymer A is the PDMS–NH_2 "block", and polymer B is the PBD–

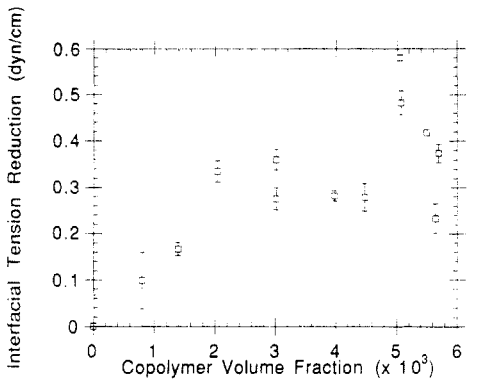

Figure 10. PBD/PBD-COOH/PDMS-NH_2/PDMS interfacial tension reduction vs copolymer volume fraction; 5.4×10^{-4} mol/L NH_2.

COOH "block". This assumes that the difunctional polymer chains are complexed through only one of the two end groups (pure diblocks). In the other extreme in which both end groups are complexed (pure multiblock), the volume fraction would be half of that given by eq 16.

It is important to determine the critical micelle volume fraction (ϕ_{cmc}) for the system, as the theory of Hong and Noolandi only applies at low copolymer concentration below the cmc. Estimating the cmc from the plateau volume fraction for the data in Figures 1–3 (applying eq 16) results in a volume fraction in the range of 0.01–0.02. Using the following equations derived by Leibler for strongly segregated systems,[36,37] ϕ_{cmc} can be calculated, where $f = N_A/N$, and μ_{cmc} is as follows:

$$\mu_{cmc} = (3/2)^{4/3} f^{4/9} (\alpha f^{-1/3} - 1)^{1/3} (\chi N)^{1/3} \quad (17)$$

$$\phi_+(\text{cmc}) = e^{\mu_{cmc} - f\chi N} \quad (18)$$

where $\alpha = 1 + 3\pi^2/40 = 1.74$. For fairly symmetric chains, $f > 0.31$, and interface saturation of the "block copolymer" will occur, whereas for asymmetric chains, $f < 0.31$ and ϕ_+(cmc) will be reached before saturation occurs. For our system $f = 0.213$, so the cmc should be observed, according to the theory. Using eqs 17 and 18, ϕ_+(cmc) is calculated as 0.0127, which is consistent with the experimental results. The interfacial tension reduction measured for the low NH_2 concentration (5.4×10^{-4} mol/L) plateaus at a volume fraction of 0.00204 as a result of the equilibrium reaction model, so this system was chosen for analysis by the block copolymer theory of Hong and Noolandi.

Interfacial tension as a function of the calculated block copolymer volume fraction for the pure diblock case is presented in Figure 10, showing that the interfacial tension decrease is approximately linear with copolymer volume fraction. A plot of interfacial tension reduction ($\Delta\gamma$) vs copolymer volume fraction (ϕ_c), as shown in Figure 10, should be linear with a slope proportional to the interfacial width, as defined by eq 15.[34] The plot is fairly linear, although at the higher concentrations there is scatter in the data.

The slope of the $\Delta\gamma$ vs ϕ_c plot provides an estimate of the interfacial width at half-height for our system. However, some approximations must be made, as our system is not perfectly symmetrical. Therefore, the geometric mean was used to calculate the average statistical segment length, b, and the "block" degree of polymerization in eq 16. If the slope of the line defined by the first six points on the curve is used, the corresponding interfacial width at half-height for the pure diblock copolymer case would be 33.0 Å. In the other extreme, pure multiblock, the calculated interfacial width would be 66.0 Å. The interfacial width would, in a real case, be somewhere between these two extremes. The predicted interfacial width for this system without block copolymer is approximately 15 Å, as calculated using the theory of Broseta et al.[39] The interfacial width would be expected to increase with block copolymer present, as has been observed by neutron reflectivity for the PS/PMMA system.[40] Therefore, the resulting interfacial width range of 33.0–66.0 Å is quite reasonable for this system.

A root-mean-square end-to-end distance ($\langle r^2 \rangle^{1/2}$) of 106 Å is calculated for the "copolymer" by summing the $\langle r^2 \rangle^{1/2}$ values for the PDMS "block" and the PBD "block". Calculation of the radius of the loop formed in the case of multiblock formation at a polymer interface, as used by Balasz et al. in Monte Carlo simulations[38] (radius = $N_b^{3/4}/\pi$), results in a radius of 65.7 Å for the PDMS chain and a radius of 36.3 Å for the PBD chain, with a total interfacial chain size of 102 Å for a multiblock copolymer case. The interfacial width at half-height should be half of the chain size and so would be expected to be within the range of 51–53 Å based on the calculations above. This range for d is consistent with that predicted by the theory of Hong and Noolandi.

Conclusions

We have demonstrated that interpolymer end-complexation across the interface between immiscible polymers is an effective means for interface modification and compatibilization of polymer blends. In many ways, the resultant interfacial tension reduction resembles that obtained when block copolymers are used as interfacial modifiers for polymer blends. The promotion of end-complexation, however, is dependent upon the equilibrium conditions regarding formation of the complex and can thus be adjusted by control of the functional group stoichiometry in the blends. The process of end group complexation is also similar to many industrial methods for blend compatibilization that are based upon in situ reactive processing. Our development of a reaction model for interpolymer end-complexation therefore represents a first step in furthering our fundamental understanding of important industrial processes such as in situ interfacial graft copolymerization in polymer blends.

Acknowledgment. This research was supported in part by the University of Connecticut Polymer Compatibilization Research Consortium, the office of Naval Research, and the National Science Foundation Polymers Program (Grant DMR-8818232). C.A.F. wishes to acknowledge support from a State of Connecticut Department of Higher Education High Technology Fellowship. The authors wish to thank Prof. Andrew Garton for helpful discussions regarding the infrared spectroscopy studies and Prof. Michael Cutlip for assistance in development of the reaction model. The authors are also grateful to Prof. Judy Riffle and Dr. Iskender Yilgor for supplying some of the materials and to Dr. Val Krukonis for fractionating some of the materials.

Appendix. Dimerization Equilibrium Constant Calculations

The extinction coefficient for the bonded carbonyl (ϵ_b) was determined at room temperature, where the free carbonyl concentration could be neglected. The extinction coefficient for the free carbonyl (ϵ_f) was assumed to be half that of the bonded carbonyl, as was determined previously.[41] This is consistent with the frequently used assumption that the extinction coefficients for the bonded

and the free carbonyl are equal, and since the dimer contains two bonded carbonyl groups, the extinction coefficient should be larger by a factor of 2. Therefore, the resulting equations for ϵ_b and K_d, as was used by MacKnight et al., would be[30]

$$\epsilon_b = \frac{2}{c_T t}(A_b + A_f) \tag{19}$$

$$K_d = \frac{[D]}{[A]^2} = \frac{A_b \epsilon_b t}{4A_f^2} \tag{20}$$

where A_b and A_f are the absorbances for the bonded and free carbonyl, respectively, t is the cell thickness, controlled by the spacer, and c_T is the total carbonyl concentration.

References and Notes

(1) Wu, S. *Polym. Eng. Sci.* **1987**, *5*, 335.
(2) Patterson, H. T.; Hu, K. H.; Grindstaff, T. H. *J. Polym. Sci.* **1971**, *34*, *31*.
(3) Gaillard, P.; Ossenbach-Sutter, M.; Reiss, G. *Makromol. Chem., Rapid Commun.* **1980**, *1*, 771.
(4) Anastasiadis, S. H.; Gancarz, I.; Koberstein, J. T. *Macromolecules* **1989**, *22*, 1449.
(5) Brown, H. R. *Macromolecules* **1989**, *22*, 2859.
(6) Creton, C.; Kramer, E. J.; Hadziioannou, G. *Macromolecules* **1991**, *24*, 1846.
(7) Fayt, R.; Jerome, R.; Teyssie, Ph. *J. Polym. Sci., Polym. Lett. Ed.* **1981**, *19*, 79.
(8) Hobbs, S. Y.; Bopp, R. C.; Watkins, V. H. *Polym. Eng. Sci.* **1983**, *23*, 380.
(9) Russell, T. P.; Jerome, R.; Charlier, P.; Foucart, M. *Macromolecules* **1988**, *21*, 1709.
(10) Sen, A.; Weiss, R. A.; Garton, A. *ACS Symp. Ser.* **1989**, *No. 395*, 353.
(11) Moskala, E. J.; Howe, S. E.; Painter, P. C.; Coleman, M. M. *Macromolecules* **1984**, *17*, 1671.
(12) Painter, P. C.; Park, Y.; Coleman, M. M. *Macromolecules* **1989**, *22*, 570.
(13) Painter, P. C.; Park, Y.; Coleman, M. M. *Macromolecules* **1989**, *22*, 580.
(14) Rutkowska, M.; Eisenberg, A. *Macromolecules* **1984**, *17*, 821.
(15) Murali, R.; Eisenberg, A. *J. Polym. Sci., Part B: Polym. Phys.* **1988**, *26*, 1385.
(16) Tsuchida, E.; Abe, K. In *Advances in Polymer Science*; Springer-Verlag: Heidelberg, Germany, 1982.
(17) Smith, P.; Hara, M.; Eisenberg, A. In *Current Topics in Polymer Science*; Ottenbrite, R., Utracki, L., Inoue, T., Eds.; Hanser: Munich, Vienna, New York, 1987; Vol. II, Chapter 6.3.
(18) Cousin, P.; Prud'homme, R.; Garton, A. In *Current Topics in Polymer Science*; Ottenbrite, R., Utracki, L., Inoue, T., Eds.; Hanser: Munich, Vienna, New York, 1987; Vol. II, Chapter 6.4.
(19) Natansohn, A.; Eisenberg, A. *Macromolecules* **1987**, *20*, 323.
(20) Rees, R. W. *Polym. Prepr. (Am. Chem. Soc., Div. Polym. Chem.)* **1973**, *14*, 796.
(21) Rees, R. W. U.S. Patent **1969**, 3 471 460.
(22) Yilgor, I.; McGrath, J. E. *Adv. Polym. Sci.* **1986**, *86*, 1.
(23) Elsbernd, C. S.; Spinu, M.; Krukonis, V. J.; Gallagher, P. M.; Mohanty, D. K.; McGrath, J. E. *Adv. Chem. Ser.* **1990**, *No. 224*, 145.
(24) Fleischer, C. A.; Koberstein, J. T.; Krukonis, V. J.; Gallagher, P. A. *Macromolecules* **1993**, *26*, 4172.
(25) Anastasiadis, S. H.; Chen, J.-K.; Koberstein, J. T.; Siegel, A. F.; Sohn, J. E.; Emerson, J. A. *J. Colloid Interface Sci.* **1987**, *119*, 55.
(26) Bhatia, Q. S.; Chen, J.-K.; Koberstein, J. T.; Sohn, J. E.; Emerson, J. A. *J. Colloid Interface Sci.* **1985**, *106*, 353.
(27) Bashforth, S.; Adams, J. C. *An. Attempt to Test the Theory of Capillary Action*; Cambridge University Press and Deighton, Bell and Co.: London, 1882.
(28) Supplied by Material Interface Associates, La Mesita Ave., Albuquerque, NM.
(29) Schacham, M. *Comput. Chem. Eng.* **1978**, *2*, 197.
(30) MacKnight, W. J.; McKenna, L. W.; Read, B. E.; Stein, R. S. *J. Chem. Phys.* **1968**, *72*, 1122.
(31) Landry, C. J. T.; Teegarden, D. M. *Macromolecules* **1991**, *24*, 4310.
(32) Schulz, D. N.; Kitano, K.; Duvdevani, I.; Kowalik, R. M.; Eckert, J. A. In *Cell Separation Science and Technology*; ACS Symposium Series 464; Schultz, D. N., Glass, J. E., Eds.; American Chemical Society: Washington, D.C., 1991.
(33) Hong, K. M.; Noolandi, J. *Macromolecules* **1981**, *14*, 727.
(34) Hong, K. M.; Noolandi, J. *Macromolecules* **1982**, *15*, 482.
(35) Noolandi, J.; Hong, K. M. *Macromolecules* **1984**, *17*, 1531.
(36) Leibler, L. *Makromol. Chem., Macromol. Symp.* **1988**, *16*, 1.
(37) Leibler, L. *Physica A* **1991**, *171*, 258.
(38) Balasz, A. C.; Siemasko, C. P.; Lantman, C. W. *J. Chem. Phys.* **1991**, *94* (2), 1653.
(39) Broseta, P.; Fredrickson, G. H.; Helfand, E.; Leibler, L. *Macromolecules* **1990**, *23*, 132.
(40) Russell, T. P.; Anastasiadis, S. H.; Menell, A.; Flecher, G. P.; Satija, S. K. *Macromolecules* **1991**, *24*, 1575.
(41) Chang, L. C.-Y. Ph.D. Thesis, Polytechnic Institute of Brooklyn, Brooklyn, NY, 1955.